

Thermal photons in QGP and non-ideal effects

Jitesh R. Bhatt,^{*} Hiranmaya Mishra,[†] and V. Sreekanth[‡]

Physical Research Laboratory, Ahmedabad 380009, India

We investigate the thermal photon production-rates using one dimensional boost-invariant second order relativistic hydrodynamics to find proper time evolution of the energy density and the temperature. The effect of bulk-viscosity and non-ideal equation of state are taken into account in a manner consistent with recent lattice QCD estimates. It is shown that the *non-ideal* gas equation of state i.e $\epsilon - 3P \neq 0$ behaviour of the expanding plasma, which is important near the phase-transition point, can significantly slow down the hydrodynamic expansion and thereby increase the photon production-rates. Inclusion of the bulk viscosity may also have similar effect on the hydrodynamic evolution. However the effect of bulk viscosity is shown to be significantly lower than the *non-ideal* gas equation of state. We also analyze the interesting phenomenon of bulk viscosity induced cavitation making the hydrodynamical description invalid. We include the viscous corrections to the distribution functions while calculating the photon spectra. It is shown that ignoring the cavitation phenomenon can lead to erroneous estimation of the photon flux.

I. INTRODUCTION

Thermal photons emitted from the hot fireball created in relativistic heavy-ion collisions is a promising tool for providing a signature of quark-gluon plasma [1–6] (see [7–9] for recent reviews). Since they participate only in electromagnetic interactions, they have a larger mean free path compared to the transverse size of the hot and dense matter created in nuclear collisions [10]. Therefore these photons were proposed to verify the existence of the QGP phase [11, 12]. Spectra of thermal photons depend upon the fireball temperature and they can be calculated from the scattering cross-section of the processes like $q\bar{q} \rightarrow g\gamma$, *bremstrahlung* etc. Time evolution of the temperature can be calculated using hydrodynamics with appropriate initial conditions. Thus the spectra depend upon the equation of state (EoS) of the medium and they may be useful in finding a signature of the quark-gluon plasma[13–16]. Recently thermal photons are proposed as a tool to measure the shear viscosity of the strongly interacting matter produced in the collisions[17, 18].

Understanding the shear viscosity of QGP is one of the most intriguing aspects of the experiments at Relativistic Heavy Ion Collider (RHIC). Analysis of the experimental data collected from RHIC shows that the strongly coupled matter produced in the collisions is not too much above the phase transition temperature T_c and it may have extremely small value of shear viscosity η . The ratio of the shear viscosity η to the entropy density s i.e. η/s is around $1/4\pi$ which is the smallest for any known liquid in the nature[19]. In fact the arguments based on AdS-CFT suggest that the values of η/s can not become

lower than $1/4\pi$. This is now known as Kovtun-Son-Starinets or 'KSS- bound' [20]. Thus the quark-gluon plasma produced in RHIC experiments is believed to be in a form of the most perfect liquid[21]. No wonder ideal hydrodynamic appears to be the best description of such matter as suggested by comparison between the experimental data[22] and the calculations done using second-order relativistic hydrodynamics [23–30].

However there remain uncertainties in understanding the application and validity of the hydrodynamical procedure in relativistic heavy-ion collision experiments. It is only very recently realized that the effect of bulk viscosity can bring complications in the hydrodynamical description of the heavy-ion collisions. Generally it was believed that the bulk viscosity, ζ does not play a significant role in the hydrodynamics of relativistic heavy-ion collisions. It was argued that that since ζ scaled like $\epsilon - 3P$ at very high energy the bulk viscosity may not play a significant role because the matter might be following the ideal gas type equation of state[31]. But during its course of expansion the fireball temperature can approach values close to T_c . Recent lattice QCD results show that the quark-gluon matter do not satisfy ideal EoS near T_c and the ratio ζ/s show a strong peak around T_c [32, 33]. The bulk viscosity contribution in this regime can be much larger than that of the shear viscosity. Recently the role of bulk viscosity in heating and expansion of the fireball was analyzed using one dimensional hydrodynamics[34]. Another complication that bulk viscosity brings in hydrodynamics of heavy-ion collisions is phenomenon of cavitation[35]. Cavitation arises when the fluid pressure becomes smaller than the vapour pressure. Since the bulk viscosity (and also shear viscosity) contributes to the pressure gradient with a negative contribution, it may be possible for the effective fluid pressure to become zero. Once the cavitation sets in, the hydrodynamical description breaks down. It was shown

^{*} jeet@prl.res.in

[†] hm@prl.res.in

[‡] skv@prl.res.in

in Ref.[35] that cavitation may happen in RHIC experiments when the effect of bulk viscosity is included in manner consistent with the lattice results. It was shown that the cavitation may significantly reduce the time of hydrodynamical evolution.

Keeping the above discussion in mind, we aim to study the effect of bulk viscosity and cavitation on the thermal photon production in heavy ion collisions. As far as we know no such study exists in the literature. Furthermore, the calculations for the photon production rates in the absence of viscous effects, are done using thermal distribution function of the particle species (e.g., quark, anti-quark etc.)[8]. However, it is well known that viscous effects can lead to the modification of the thermal distribution functions[36]. This may have observational effect on the photon spectra[18]. In this work we incorporate the viscous modification in the distribution function arising due to bulk and shear viscosities. Finite ζ effect can either significantly reduce the time for the hydrodynamical evolution (by onset of cavitation) or it can increase the time by which the system reaches T_c . Moreover the *non-ideal* gas EoS can also significantly influence the hydrodynamics. In what follows, we use equations of relativistic second order hydrodynamics to incorporate the effects of finite viscosity. We take the value of ζ/s same as that in Ref.[35] and keep $\eta/s = 1/4\pi$. Further we use one dimensional boost invariant hydrodynamics in the same spirit as in Refs.[34, 35]. One of the limitations of this approach is that the effects of transverse flow cannot be incorporated. As the boost-invariant hydrodynamics is known to lead to under-estimation of the effects of bulk viscosity[34], we believe that our study of the photon spectra will provide a conservative estimate of the effect. However it should also be noted that the effect of transverse flow could remain small as cavitation can restrict the time for hydrodynamical evolution.

II. FORMALISM

A. Viscous Hydrodynamics

We represent the energy momentum tensor of the dissipative QGP formed in high energy nuclear collisions as

$$T^{\mu\nu} = \varepsilon u^\mu u^\nu - P \Delta^{\mu\nu} + \Pi^{\mu\nu} \quad (1)$$

where ε , P and u^μ are the energy density, pressure and four velocity of the fluid element respectively. The operator $\Delta^{\mu\nu} = g^{\mu\nu} - u^\mu u^\nu$ acts as a projection perpendicular to four velocity. The viscous contributions to $T^{\mu\nu}$ are represented by

$$\Pi^{\mu\nu} = \pi^{\mu\nu} - \Delta^{\mu\nu} \Pi \quad (2)$$

where $\pi^{\mu\nu}$, the traceless part of $\Pi^{\mu\nu}$; gives the contribution of shear viscosity and Π gives the bulk viscosity

contribution. The corresponding hydrodynamics equations are given by,

$$D\varepsilon + (\varepsilon + P) \Theta - \Pi^{\mu\nu} \nabla_{(\mu} u_{\nu)} = 0 \quad (3)$$

$$(\varepsilon + P) Du^\alpha - \nabla^\alpha P + \Delta_{\alpha\nu} \partial_\mu \Pi^{\mu\nu} = 0 \quad (4)$$

where $D \equiv u^\mu \partial_\mu$, $\Theta \equiv \partial_\mu u^\mu$, $\nabla_\alpha = \Delta_{\mu\alpha} \partial^\mu$ and $A_{(\mu} B_{\nu)} = \frac{1}{2}[A_\mu B_\nu + A_\nu B_\mu]$ gives the symmetrization.

We employ Bjorken's prescription[37] to describe the one dimensional boost invariant expanding flow, where we use the convenient parametrization of the coordinates using the proper time $\tau = \sqrt{t^2 - z^2}$ and space-time rapidity $y = \frac{1}{2} \ln[\frac{t+z}{t-z}]$; $t = \tau \cosh y$ and $z = \tau \sinh y$. Then the four velocity is given by,

$$u^\mu = (\cosh y, 0, 0, \sinh y). \quad (5)$$

We note that with this transformation of the coordinates, $D = \frac{\partial}{\partial \tau}$ and $\Theta = 1/\tau$.

Form of the energy momentum tensor in the local rest frame of the fireball is then given by[38–41]:

$$T^{\mu\nu} = \begin{pmatrix} \varepsilon & 0 & 0 & 0 \\ 0 & P_\perp & 0 & 0 \\ 0 & 0 & P_\perp & 0 \\ 0 & 0 & 0 & P_z \end{pmatrix} \quad (6)$$

where the effective pressure of the expanding fluid in the transverse and longitudinal directions are respectively given by

$$\begin{aligned} P_\perp &= P + \Pi + \frac{1}{2}\Phi \\ P_z &= P + \Pi - \Phi \end{aligned} \quad (7)$$

Here Φ and Π are the non-equilibrium contributions to the equilibrium pressure P coming from shear and bulk viscosities respectively. Respecting the symmetries in the transverse directions the traceless shear tensor has the form $\pi^{ij} = \text{diag}(\Phi/2, \Phi/2, -\Phi)$.

In the first order Navier-Stokes dissipative hydrodynamics

$$\Pi = -\zeta \partial_\mu u^\mu \quad \text{and} \quad \pi^{\mu\nu} = \eta \nabla^{(\mu} u^{\nu)}, \quad (8)$$

with $\zeta, \eta > 0$ and $\nabla_{(\mu} u_{\nu)} = 2\nabla_{(\mu} u_{\nu)} - \frac{2}{3} \Delta_{\mu\nu} \nabla_\alpha u^\alpha$. So for first order theories with Bjorken flow we have

$$\Pi = -\frac{\zeta}{\tau} \quad \text{and} \quad \Phi = \frac{4\eta}{3\tau}. \quad (9)$$

The Navier-Stokes hydrodynamics is known to have instabilities and acausal behaviours[42, 43]—second order theories removes such unphysical artifacts.

We use causal dissipative second order hydrodynamics of Israel-Stewart[44] to study the expanding plasma in the fireball. In this theory we have evolution equations for Π and Φ governed by their relaxation times τ_Π and

τ_π . We refer [45, 46] for more details on the recent developments in the theory and its application to relativistic heavy ion collisions.

Under these assumptions, the set of equations (i.e., equation of motion (3) and relaxation equations for viscous terms) dictating the longitudinal expansion of the medium are given by [40, 43, 47]

$$\frac{\partial \varepsilon}{\partial \tau} = -\frac{1}{\tau}(\varepsilon + P + \Pi - \Phi), \quad (10)$$

$$\frac{\partial \Phi}{\partial \tau} = -\frac{\Phi}{\tau_\pi} + \frac{2}{3} \frac{1}{\beta_2 \tau} - \left[\frac{4\tau_\pi}{3\tau} \Phi + \frac{\lambda_1}{2\eta^2} \Phi^2 \right], \quad (11)$$

$$\frac{\partial \Pi}{\partial \tau} = -\frac{\Pi}{\tau_\Pi} - \frac{1}{\beta_0 \tau}. \quad (12)$$

where $\Phi = \pi^{00} - \pi^{zz}$. The terms in the square bracket in Equation (11) are needed for the conformality of the theory [48]. The coefficients β_0 and β_2 are related with the relaxation time by

$$\tau_\Pi = \zeta \beta_0, \tau_\pi = 2\eta \beta_2. \quad (13)$$

We use the $\mathcal{N} = 4$ supersymmetric Yang-Mills theory expressions for τ_π and λ_1 [48–50]:

$$\tau_\pi = \frac{2 - \ln 2}{2\pi T} \quad (14)$$

and

$$\lambda_1 = \frac{\eta}{2\pi T}. \quad (15)$$

We set $\tau_\pi(T) = \tau_\Pi(T)$ as we don't have any reliable prediction for τ_Π [34].

In order to close the hydrodynamical evolution equations (10 - 12) we need to supply the EoS.

B. Equation of state, ζ/s and η/s

We are interested in the effect of bulk viscosity on the hydrodynamical evolution of the plasma and recent studies show that near the critical temperature T_c effect of bulk viscosity becomes important [51–55]. We use the recent lattice QCD result of A. Bazavov *et al.* [32] for equilibrium equation of state (EoS) (*non-ideal*: $\varepsilon - 3P \neq 0$). Parametrised form of their result for trace anomaly is given by

$$\frac{\varepsilon - 3P}{T^4} = \left(1 - \frac{1}{\left[1 + \exp\left(\frac{T - c_1}{c_2}\right) \right]^2} \right) \left(\frac{d_2}{T^2} + \frac{d_4}{T^4} \right), \quad (16)$$

where values of the coefficients are $d_2 = 0.24 \text{ GeV}^2$, $d_4 = 0.0054 \text{ GeV}^4$, $c_1 = 0.2073 \text{ GeV}$, and $c_2 = 0.0172 \text{ GeV}$ [35]. Their calculations predict a crossover from QGP to

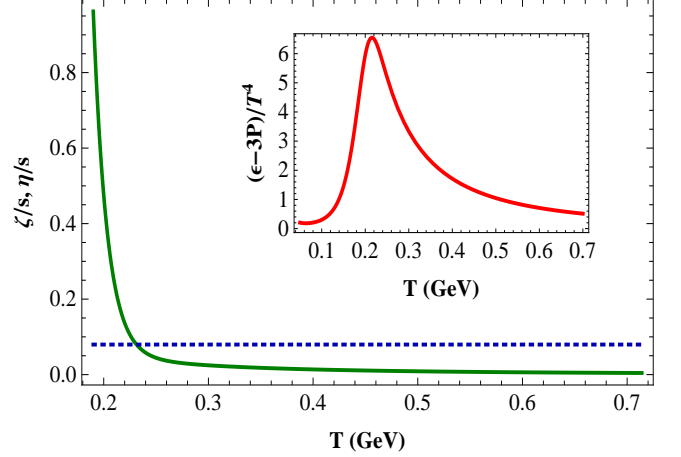


FIG. 1. $(\varepsilon - 3P)/T^4$, ζ/s (and $\eta/s = 1/4\pi$) as functions of temperature T . One can see around critical temperature ($T_c = .190 \text{ GeV}$) $\zeta \gg \eta$ and departure of equation of state from ideal case is large.

hadron gas around 0.2-0.18 GeV. We take critical temperature T_c as 0.19 GeV throughout the analysis. The functional form of the pressure is given by [32]

$$\frac{P(T)}{T^4} - \frac{P(T_0)}{T_0^4} = \int_{T_0}^T dT' \frac{\varepsilon - 3P}{T'^5}, \quad (17)$$

with $T_0 = 50 \text{ MeV}$ and $P(T_0) = 0$ [35].

From Equations (16) and (17) we get ε and P in terms of T .

We rely upon the lattice QCD calculation results for determining ζ/s . We use the result of Meyer [33], which indicate the existence a peak of ζ/s near T_c , however the height and width of this curve are not well understood. We follow parametrization of Meyer's result from Ref. [35], given by

$$\frac{\zeta}{s} = a \exp\left(\frac{T_c - T}{\Delta T}\right) + b \left(\frac{T_c}{T}\right)^2 \quad \text{for } T > T_c, \quad (18)$$

where $b = 0.061$. The parameter a controls the height and ΔT controls the width of the ζ/s curve and are given by

$$a = 0.901, \Delta T = \frac{T_c}{14.5}. \quad (19)$$

We will change these values to explore the various cases of ζ/s to account for the uncertainty of the height and width of the curve.

We use the lower bound of the shear viscosity to entropy density ratio known as KSS bound [20]

$$\eta/s = 1/4\pi \quad (20)$$

in our calculations. We note that the entropy density is obtained from the relation

$$s = \frac{\varepsilon + P}{T}. \quad (21)$$

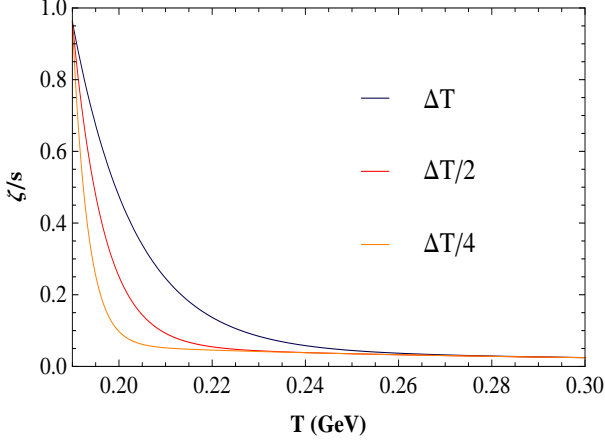


FIG. 2. Various bulk viscosity scenarios by changing the width of the curve through the parameter ΔT .

In Fig.[1] we plot the trace anomaly $(\varepsilon - 3P)/T^4$ and ζ/s for desired temperature range. We also plot the constant value of $\eta/s = 1/4\pi$ for a comparison. It is clear that the *non-ideal* EoS deviates from the *ideal* case ($\varepsilon = 3P$) significantly around the critical temperature. Around same temperature ζ/s starts to dominate over η/s significantly. We would like to note that these results are qualitatively in agreement with Ref.[34].

In Fig.[2] we show the change in bulk viscosity profile by varying the width of the ζ/s curve by keeping the height intact.

C. Thermal photons

During QGP phase thermal photons are originated from various sources, like *Compton scattering* $q(\bar{q})g \rightarrow q(\bar{q})\gamma$ and annihilation processes $q\bar{q} \rightarrow g\gamma$. Recently Au-

renche *et al.* showed that two loop level *bremsstrahlung* process contribution to photon production is as important as *Compton* or *annihilation* contributions evaluated up to one loop level[56]. They also discussed a new mechanism for hard photon production through the annihilation of an off-mass shell quark and an antiquark, with the off-mass shell quark coming from scattering with another quark or gluon. These processes in the context of hydrodynamics of heavy ion collisions were studied in Refs.[13, 14]. Until recently only the processes of *Compton scattering* and $q\bar{q}$ -*annihilation* were considered in studying the photon production rates.

The production rate for hard ($E > T$) thermal photons from equilibrated QGP evaluated to the one loop order using perturbative thermal QCD based on hard thermal loop (HTL) resummation to account medium effects. The *Compton scattering* and $q\bar{q}$ -*annihilation* contribution to the photon production rate is[1, 2, 5]

$$E \frac{dN}{d^4x d^3p} = \frac{1}{2\pi^2} \alpha \alpha_s \left(\sum_f e_f^2 \right) T^2 e^{-E/T} \ln \left(\frac{cE}{\alpha_s T} \right), \quad (22)$$

where the constant $c \approx 0.23$ and α and α_s are the electromagnetic and strong coupling constants respectively. In the summation f is over the flavours of the quarks and e_f is the electric charge of the quark in units of the charge of the electron.

The rate of photon production due to *Bremsstrahlung* processes is given by[56]

$$E \frac{dN}{d^4x d^3p} = \frac{8}{\pi^5} \alpha \alpha_s \left(\sum_f e_f^2 \right) \frac{T^4}{E^2} e^{-E/T} (J_T - J_L) I(E, T), \quad (23)$$

where $J_T \approx 1.11$ and $J_L \approx 1.06$ for two flavours and three colors of quarks[14]. The expression for $I(E, T)$ is given by

$$I(E, T) = \left[3\zeta(3) + \frac{\pi^2 E}{6 T} + \left(\frac{E}{T} \right)^2 \ln(2) + 4 \text{Li}_3 \left(-e^{-|E|/T} \right) + 2 \left(\frac{E}{T} \right) \text{Li}_2 \left(-e^{-|E|/T} \right) - \left(\frac{E}{T} \right)^2 \ln \left(1 + e^{-|E|/T} \right) \right], \quad (24)$$

where Li are the polylogarithmic functions given by

$$\text{Li}_a(z) = \sum_{n=1}^{+\infty} \frac{z^n}{n^a}.$$

Next the rate due to $q\bar{q}$ -*annihilation with an additional*

scattering in the medium is given by,

$$E \frac{dN}{d^4x d^3p} = \frac{8}{3\pi^5} \alpha \alpha_s \left(\sum_f e_f^2 \right) E T e^{-E/T} (J_T - J_L). \quad (25)$$

We use the parametrization of $\alpha_s(T)$ by Karsch[57]:

$$\alpha_s(T) = \frac{6\pi}{(33 - 2N_f) \ln(8T/T_c)} \quad (26)$$

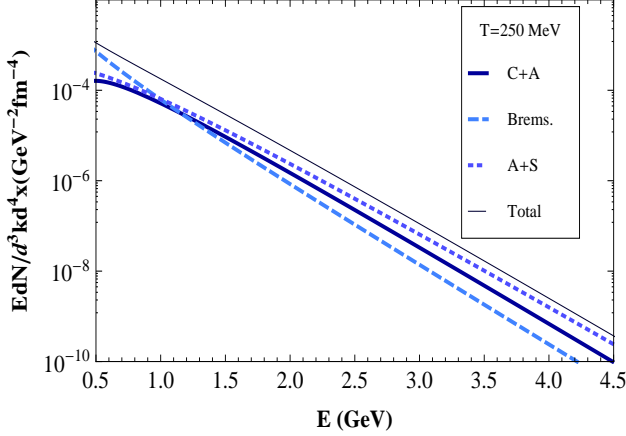


FIG. 3. Hard thermal photon rates in QGP as a function of energy for a fixed temperature $T=250$ MeV. Photon rates are plotted for different relevant processes.

for our rate calculations. Here N_f is the number of quark flavors in consideration.

In Fig.[3], we plot the different photon rates for a fixed temperature $T = 250$ MeV. It shows the contributions from *Bremsstrahlung* (Brems), *annihilation with scattering* (A+S) and *Compton scattering* together with *q \bar{q} -annihilation* (C+A). *Bremsstrahlung* contributes to the photon production rate upto $E \sim 1$ GeV only, afterwards A+S and C+A processes become dominant. We might mention here that this observation is in agreement with Ref.[14].

The total photon rate is obtained by adding different temperature depended photon rate expressions. Once the evolution of temperature is known from the hydrodynamical model, the *total photon spectrum* is obtained by integrating the total rate over the space time history of the collision[58],

$$\begin{aligned} \left(\frac{dN}{d^2p_T dy} \right)_{y,p_T} &= \int d^4x \left(E \frac{dN}{d^3pd^4x} \right) \\ &= Q \int_{\tau_0}^{\tau_1} d\tau \tau \int_{-y_{nuc}}^{y_{nuc}} dy' \left(E \frac{dN}{d^3pd^4x} \right) \end{aligned} \quad (27)$$

where τ_0 and τ_1 are the initial and final values of time we are interested. y_{nuc} is the rapidity of the nuclei whereas Q is its transverse cross-section. For a Au nucleus $Q \sim 180 fm^2$. p_T is the photon momentum in direction perpendicular to the collision axis. The quantity $\left(E \frac{dN}{d^3pd^4x} \right)$ is Lorentz invariant and it is evaluated in the local rest frame in equation (27). Now the photon energy in this frame, i.e., in the frame comoving with the plasma, is given as $p_T \cosh(y - y')$. So once the rapidity and p_T are given we get the total photon spectrum.

D. Viscous corrections to the distribution functions

Viscous effects contribute in two ways in kinetic theory: Firstly, it can change the width (temperature) of the distribution function. Secondly, it can modify the momentum dependence of the distribution function. The first effect is incorporated when we calculate the temperature as a function of time using dissipative hydrodynamics. To include the second effect one needs to compute the change in the distribution function as a function of momentum using the techniques of kinetic theory[36]. In the following we give some details of such a calculation.

In section II C, while writing the photon rates, we have used Boltzmann distribution function of type $f = f_0 = e^{-pu/T}$. In order to incorporate the modification due to viscous effects we write the distribution function as $f = f_0 + \delta f$, with $\delta f = \delta f_\eta + \delta f_\zeta$, where δf_η and δf_ζ represent change in the distribution function due to shear and bulk viscosity respectively. We calculate δf using 14-moment Grad's method. It ought to be mentioned that recent results show that calculation of δf using this method fails near freezeout region by making δf even larger than f_0 and $f < 0$ [59–61]. It is therefore important to here that we are applying these corrections to calculate the photon production rate of hard thermal photons in the regime $T > T_c$. We have found that for p_T below 3 GeV, this approximation is reasonable but beyond it, this approximation breaks down as the contribution arising from the viscous correction δf to the distribution function becomes larger than f_0 [62]. With this caveat we proceed to calculate δf applying the techniques used in Refs.[25, 38].

We write the viscous correction to the (Boltzmann) distribution function as

$$\begin{aligned} f(p) &= f_0 + \delta f = f_0 + \delta f_\eta + \delta f_\zeta \\ &= f_0 \left(1 + \frac{C}{2T^3} p^\alpha p^\beta \nabla_{\langle \alpha} u_{\beta \rangle} + \frac{A}{2T^3} p^\alpha p^\beta \Delta_{\alpha\beta} \Theta \right) \end{aligned} \quad (28)$$

where we restrict the corrections to f upto quadratic order in momentum. In order to find the coefficients A and C we first express the energy momentum tensor using f ,

$$\begin{aligned} T^{\mu\nu} &= \int \frac{d^3p}{(2\pi)^3 E} p^\mu p^\nu f \\ &= T_o^{\mu\nu} + \eta \nabla^{\langle \mu} u^{\nu \rangle} + \zeta \Delta^{\mu\nu} \Theta, \end{aligned} \quad (29)$$

so that we have

$$\eta \nabla^{\langle \mu} u^{\nu \rangle} = \frac{C}{2T^3} \left[\int \frac{d^3p}{(2\pi)^3 E} p^\mu p^\nu p^\alpha p^\beta f_o \right] \nabla_{\langle \alpha} u_{\beta \rangle}, \quad (30)$$

$$\zeta \Delta^{\mu\nu} \Theta = \frac{A}{2T^3} \left[\int \frac{d^3p}{(2\pi)^3 E} p^\mu p^\nu p^\alpha p^\beta f_o \right] \Delta_{\alpha\beta} \Theta. \quad (31)$$

Now from Eq.[30] we get the correction δf_η due to the shear viscosity as given in Ref.[38] by finding out C and

we will not repeat that calculation here. Next we will find out the coefficient A by constructing a fourth rank symmetric tensor out of $\Delta^{\mu\nu}$ and u^μ representing the term in square brackets in Eq.[31],

$$\begin{aligned} \frac{A}{2T^3} \left[\int \frac{d^3p}{(2\pi)^3 E} p^\mu p^\nu p^\alpha p^\beta f_o \right] &= a_o (u^\mu u^\nu u^\alpha u^\beta) \quad (32) \\ &+ a_1 (\Delta^{\mu\nu} u^\alpha u^\beta + \text{permutations}) \\ &+ a_2 (\Delta^{\mu\nu} \Delta^{\alpha\beta} + \Delta^{\mu\alpha} \Delta^{\nu\beta} + \Delta^{\mu\beta} \Delta^{\nu\alpha}) . \end{aligned}$$

Now substituting this expression in Eq. [31] and by noting $\Delta_{\mu\nu} u^\nu = 0$, $\Delta_{\mu\nu} \Delta^{\mu\nu} = 3$ and $\Delta^{\mu\nu} \Delta_{\mu\alpha} = \Delta_{\alpha}^\nu$ we get $\zeta = 5a_2$. Now by contracting both sides of Eq. [32] with $\frac{1}{45} (\Delta_{\mu\nu} \Delta_{\alpha\beta} + \Delta_{\mu\alpha} \Delta_{\nu\beta} + \Delta_{\mu\beta} \Delta_{\nu\alpha})$ we get,

$$\frac{A}{2T^3} \int \frac{d^3p}{(2\pi)^3 E} f_o \frac{3}{45} [p^2 - (u \cdot p)^2] = a_2 = \zeta/5. \quad (33)$$

Evaluating this expression in the local rest frame of the fluid $u^\mu = (1, \vec{0})$ we get

$$\zeta = \frac{1}{3} \frac{A}{2T^3} \int \frac{d^3p}{(2\pi)^3 E} f_o |\mathbf{p}|^4. \quad (34)$$

Now for a Boltzmann gas with $f_o = e^{-pu/T}$ we can calculate the integral and comparing the result with that of the entropy density s of an ideal boson gas[38] we find, $A = \frac{2}{5} \zeta/s$. So the viscous correction to the distribution function due to both shear [38] and bulk viscosities are given as

$$f = f_o \left(1 + \frac{\eta/s}{2T^3} p^\alpha p^\beta \nabla_{\langle\alpha} u_{\beta\rangle} + \frac{2}{5} \frac{\zeta/s}{2T^3} p^\alpha p^\beta \Delta_{\alpha\beta} \Theta \right). \quad (35)$$

Using the Bjorken's flow one can calculate $\nabla_{\langle\alpha} u_{\beta\rangle}$ and $\Delta_{\alpha\beta} \Theta$ for the present problem. Four velocity can be written as $u^\alpha = (\cosh y', 0, 0, \sinh y')$, where y' is the rapidity. Let the four momentum of a particle be parametrised as $p^\alpha = (m_T \cosh y, p_T \cos \phi_p, p_T \sin \phi_p, m_T \cosh y)$, where $m_T^2 = p_T^2 + m^2$ [38].

Finally we write the distribution function including viscous correction as

$$\begin{aligned} f = f_o \left(1 + \frac{\eta/s}{2T^3} \left[\frac{2}{3\tau} p_T^2 - \frac{4}{3\tau} m_T^2 \sinh^2(y - y') \right] \right. \\ \left. - \frac{2}{5} \frac{\zeta/s}{2T^3} \left[\frac{p_T^2}{\tau} + \frac{m_T^2}{\tau} \sinh^2(y - y') \right] \right). \end{aligned} \quad (36)$$

This expression for distribution function will be used in estimating the photon production rates in Eq.[27].

III. RESULTS AND DISCUSSION

In order to understand the temporal evolution of temperature $T(\tau)$, pressure $P(\tau)$ and viscous stresses -

TABLE I. Initial conditions for RHIC

y_{nuc}	τ_0	T_0
$(fm/c) (GeV)$		
5.3	0.5	.310

$\Phi(\tau)$ and $\Pi(\tau)$, we numerically solve the hydrodynamical equations describing the longitudinal expansion of the plasma: Eqs.[10-12]. We use the *non-ideal* EoS obtained from Eq.[16] and Eq.[17]. Information about viscosity coefficients ζ and η are obtained from Eqs.[18-20] using Eq.[21]. We need to specify the initial conditions to solve the hydrodynamical equations, namely the initial time τ_0 and T_0 . We use the initial values relevant for RHIC experiment given in Table I, taken from Ref.[13]. We will take initial values of viscous contributions as $\Phi(\tau_0) = 0$ and $\Pi(\tau_0) = 0$. We would like to note that our hydrodynamical results are in agreement with that of Ref.[35].

Once we get the temperature profile we calculate the photon production rates. Total photon spectrum $E \frac{dN}{d^3p d^4x}$ (as a function of rapidity, y and transverse momentum of photon, p_T) is obtained by adding different photon rates using Eqs. [22,23,25] and convoluting with the space time evolution of the heavy-ion collision with Eq.[27]. The final value of time τ_1 is the time at which temperature evolves to critical value τ_f , i.e.; $T(\tau_1) = T_c$. In all calculations we will consider the photon production in mid-rapidity region ($y = 0$) only.

We will be exploring various values of viscosity and its effect on the system. Since there is an ambiguity regarding the height and width of ζ/s curve, we will vary the parameters a and ΔT from its base value given in Eq.[19]. By this we will be able to study the effect of variation of ζ on the system. The varied values of the parameters are represented by a' and $\Delta T'$. We note that unless specified we will be using the base values of bulk viscosity parameters (from Eq.[19]) in our calculations. Throughout the analysis we will keep the shear viscosity η to its base value given by Eq.[20].

In order to understand the effect of *non-ideal* EoS in hydrodynamical evolution and subsequent photon spectra we compare these results with that of an *ideal* EoS ($\varepsilon = 3P$). We consider the EoS of a relativistic gas of massless quarks and gluons. The pressure of such a system is given by

$$P = a T^4; a = \left(16 + \frac{21}{2} N_f \right) \frac{\pi^2}{90} \quad (37)$$

where $N_f = 2$ in our calculations. Hydrodynamical evolution equations of such an EoS within ideal (without viscous effects) Bjorken flow can be solved analytically

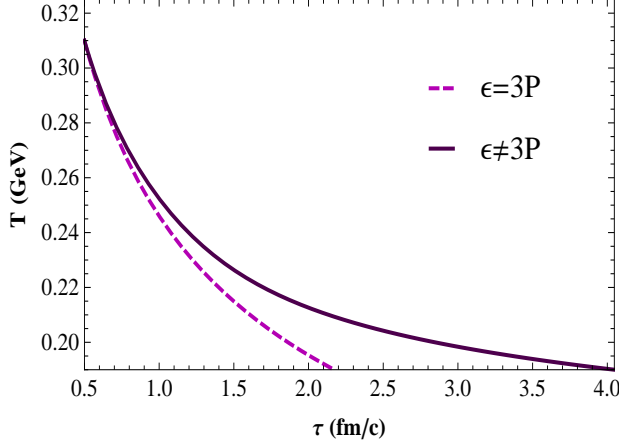


FIG. 4. Temperature profile using massless (*ideal*) and *non-ideal* EoS in RHIC scenario. Viscous effects are neglected in both cases. System evolving with *non-ideal* EoS takes a significantly larger time to reach T_c as compared to *ideal* EoS scenario.

and the temperature dependence is given by[37]

$$T = T_0 \left(\frac{\tau_0}{\tau} \right)^{1/3}, \quad (38)$$

where τ_0 and T_0 are the initial time and temperature. While considering the viscous effect of this *ideal* EoS, we will solve the set of hydrodynamical equations (10 - 11), since effect of bulk viscosity can be neglected in the relativistic limit when the equation of state $P = \varepsilon/3$ is obeyed [31].

Hydrodynamics with *non-ideal* and *ideal* EoS

Fig.[4] shows plots of temperature versus time for the *ideal* and *non-ideal* equation of states. The temperature profiles are obtained from the hydrodynamics without incorporating the effect of viscosity. The figure shows system with *non-ideal* EoS takes almost the double time than the system with *ideal* massless EoS to reach T_c . So even when the effect of viscosity is not considered, inclusion of the *non-ideal* EoS makes significant change in temperature profile of the system. This can affect the corresponding photon production rates.

Next we analyse the viscous effects on the temperature profile. The role of shear viscosity in the boost invariant hydrodynamics of heavy ion collisions, for a chemically nonequilibrated system, was already considered in Ref.[17]. We consider possible combinations of Φ and Π in *non-ideal* EoS case and study the corresponding temperature profiles as shown in Fig.[5]. As expected viscous effects is slowing down temperature evolution. For the case of non zero bulk and shear viscosities

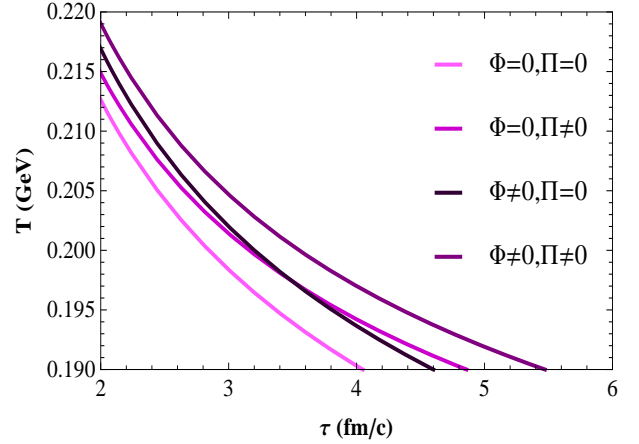


FIG. 5. Figure shows time evolution of temperature with *non-ideal* EoS for different combinations of bulk (Π) and shear (Φ) viscosities. Non zero value of bulk viscosity refers to Eqs.[18-19] and non zero shear viscosity is calculated from Eq.[20].

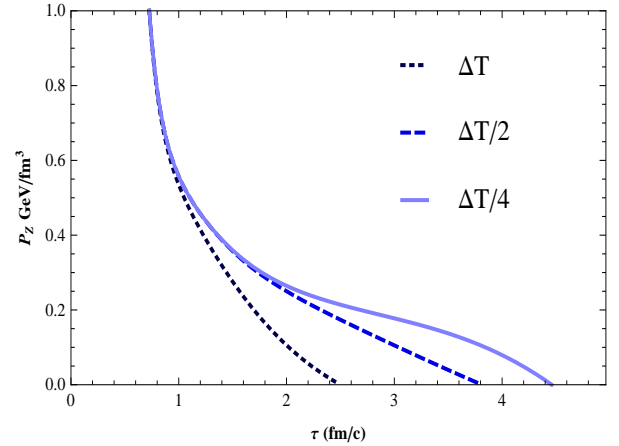


FIG. 6. Longitudinal pressure P_z for various viscosity cases shown in Fig.[2].

($\Pi \neq 0$; $\Phi \neq 0$), temperature takes the longest time to reach T_c as indicated by the top most curve. This is about 35% larger than the case without viscosity (the lowest curve). The remaining two curves show that the bulk viscosity dominates over the shear viscosity when the value of T approaches T_c and this makes the system to spend more time around T_c . However the intersection point of the two curves may vary with values of a and ΔT as highlighted by Fig.[2].

Non-ideal EoS and Cavitation

Let us note here the fact that, the bulk viscosity contribution Π is negative[35]. From the definition of lon-

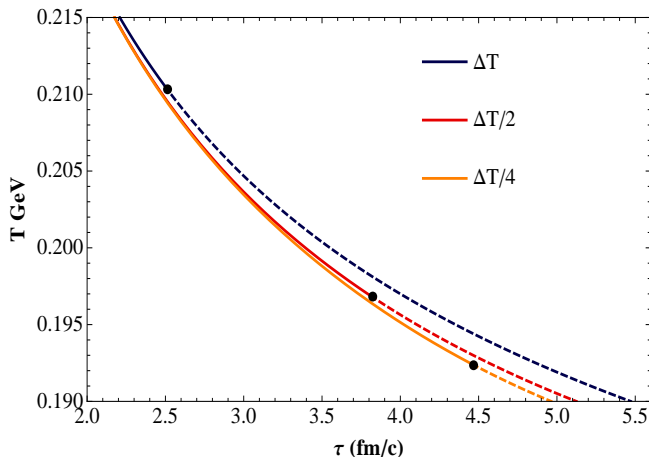


FIG. 7. Temperature is plotted as a function of time. With peak value (a) of ζ/s remains same while width (ΔT) varies. In all the three curves, solid lines end at cavitation time τ_c denoted by a dark circle. The dashed lines in each curves show how the system would evolve till T_c if cavitation is ignored. Figure shows that larger the width parameter shorter the cavitation time.

gitudinal pressure $P_z = P + \Pi - \Phi$ it is clear that if either Π or Φ is large enough it can drive P_z to negative values. $P_z = 0$ defines the condition for the onset of *cavitation*. During the course of expansion when P_z vanishes, the fluid will break apart into fragments and the hydrodynamic treatment will become invalid (see for e.g., Ref.[35]). Recent experiments at RHIC suggest η/s to its smallest value $\sim 1/4\pi$. Such a small value of η/s alone is inadequate to induce cavitation. Therefore we vary the bulk viscosity values by changing a and ΔT to study the effect cavitation. In the discussion that follows we will use τ_c to denote the time when cavitation occurs.

In Figs.[6-7] we plot P_z and T as functions of the proper time for different values of ΔT while keeping a ($=0.901$) fixed. As may be inferred from Fig.[6], higher value of ΔT leads to a shorter cavitation time. For the values of a and ΔT given by Eq.[19] we find that around $\tau_c = 2.5 \text{ fm/c}$, P_z becomes zero as shown by the lowest curve in Fig.[6]. In this case, the cavitation occurs when the temperature reaches the value about 210 MeV, as may be seen in Fig.[7]. Had we ignored the cavitation, the system would have taken a time $\tau_f = 5.5 \text{ fm/c}$ to reach T_c , which is significantly larger than τ_c . This shows that cavitation occurs rather abruptly without giving any sign in the temperature profile of the system. The hydrodynamic evolution without implementing the cavitation constraint can lead to over-estimation of the evolution time and the photon production.

We have carried out a similar analysis shown in Figs.[6-7] by keeping ΔT fixed ($= T_c/14.5$) and varying parameter a . In Fig.[8] we show the cavitation times corresponding to changes in a and ΔT (denoted by a' and

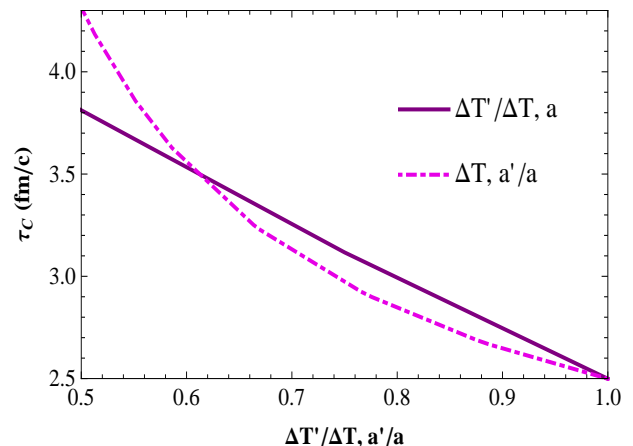


FIG. 8. Cavitation time τ_c as a function of different values of height (a') and width ($\Delta T'$) of ζ/s curve.

$\Delta T'$). The dashed curve in Fig.[8] shows τ_c as a function of a , while keeping ΔT fixed. The curve shows that τ_c decreases with increasing a . Solid line shows how τ_c varies while keeping a fixed and changing ΔT .

Thermal Photon Production

We have already seen that the calculation of photon production rates require the initial time τ_0 , final time τ_1 and $T(\tau)$. τ_1 and $T(\tau)$ are determined from the hydrodynamics. Generally τ_1 is taken as the time taken by the system to reach T_c , i.e.; τ_f . Since hydrodynamics ceases to be valid beyond the cavitation time, we must set $\tau_1 = \tau_c$. Thus photon production from QGP will be influenced by cavitation, temperature profile and *non-ideal* EoS near T_c .

Fig.[9] shows the photon production rate calculated using *ideal* (massless) and *non-ideal* EoS. The figure shows that *non-ideal* EoS case can yield significantly larger photon flux as compared to the *ideal* EoS. At $p_T = 1 \text{ GeV}$, photon flux for the *non-ideal* EoS is about 60% larger than that of *ideal* EoS case. This is because the calculation of the photon flux is done by performing time integral over the interval between the initial time τ_0 and the final time τ_1 . τ_0 is same for both the system while the τ_1 for the case with *non-ideal* EoS is two times larger than the *ideal* EoS, as may be seen in Fig.[4]. Further, since the *non-ideal* EoS allows the system to have consistently higher temperature over a longer period as compared to the massless *ideal-gas* EoS, more photons are produced.

Next, we consider the question that how the cavitation can affect the photon production rate. We emphasize that the rates should only be integrated up to the cavitation time τ_c . Fig.[10] shows the case when there is no viscous correction to the distribution function. In the

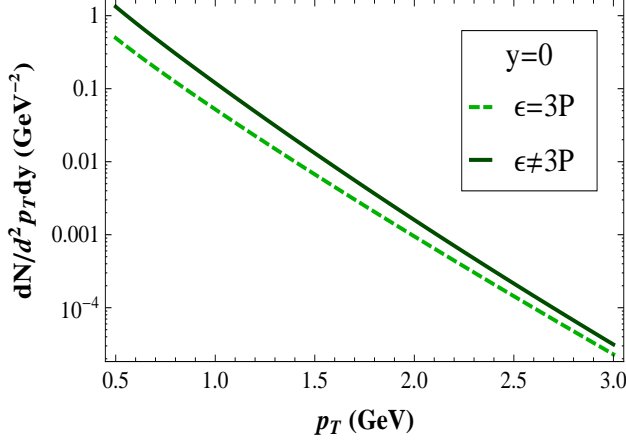


FIG. 9. Photon flux as function of transverse momentum for different equation of states. No effect of viscosity included in the hydrodynamical equations and in the distribution functions.

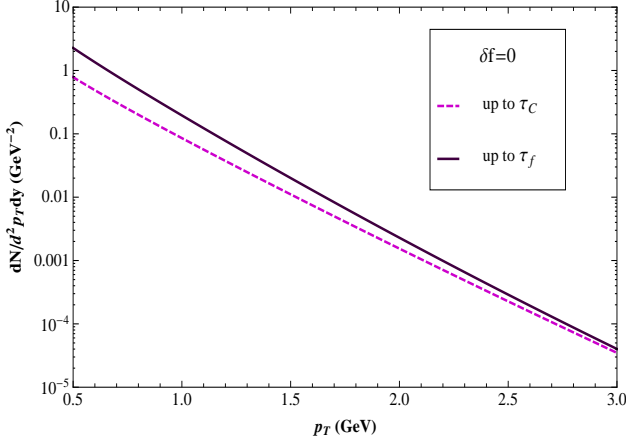


FIG. 10. Photon spectrum obtained by considering the effect of cavitation (dashed line). For a comparison we plot the spectrum without incorporating the effect of cavitation (solid line). Viscous correction to the distribution function is not considered.

dashed curve the effect of cavitation is taken into account and $\tau_1 = \tau_c = 2.5 \text{ fm}/c$. The solid line represents the same case but without the effect of the cavitation and $\tau_1 = \tau_f = 5.5 \text{ fm}/c$. It can be seen from the curve that ignoring cavitation leads to an over-estimation of the rate by about 200% at $p_T = 0.5 \text{ GeV}$ and about 50% at $p_T = 2 \text{ GeV}$. It is thus clear that the information about the cavitation time is crucial for correctly estimating thermal photon production rate.

Fig.[11] shows the similar comparison between cavitation and no-cavitation cases as in Fig.[10], but with the inclusion of viscous correction to the distribution function. The solid curve shows the case when cavitation

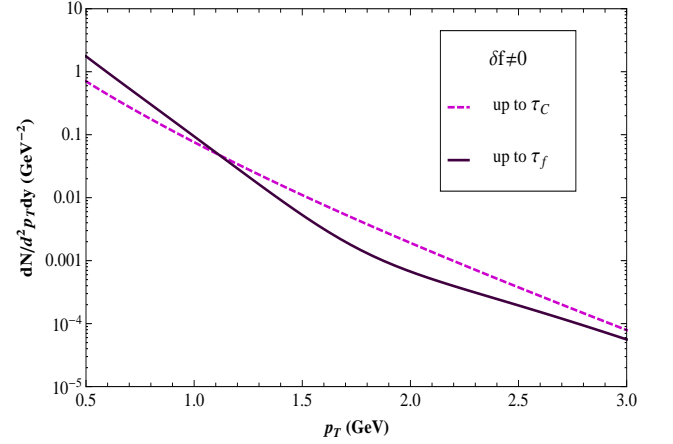


FIG. 11. Same as in Fig.[10] but with incorporating viscous correction to the distribution function.

is ignored. The dashed curve shows the effect of cavitation. First we note that as can be seen from Fig.[1], $\zeta/s \gg \eta/s$ near T_c , while η/s dominates over ζ/s when $T \gg T_c$. If one ignores the cavitation effect, then the hydrodynamical code can allow for temperature to evolve upto T_c . Moreover, we have also observed that δf_ζ contribution dominates over δf_η contribution for $p_T < 1.5 \text{ GeV}$ (A similar behaviour is reported in the Ref.[62]). Let us first note that for $\delta f = 0$, the photon flux without cavitation is higher as compared the same with cavitation at the starting p_T ($\sim 0.5 \text{ GeV}$). This feature also continues when $\delta f \neq 0$ as can be seen in Fig.[11]. The negative contribution of δf_ζ on the curve without cavitation (solid curve) makes it plummet faster than the curve with cavitation with increasing p_T (dashed curve) and both the curves intersect at $p_T \sim 1.1 \text{ GeV}$. Beyond this, the shear viscosity starts becoming more effective and prevents this faster plummet of the solid curve. Moreover, δf_ζ contribution dominates at $p_T < 1.5 \text{ GeV}$. Thus in the regime $p_T < 1.5$, ignoring the cavitation effect can lead to over-estimation of the photon flux; e.g., at $p_T = 0.5 \text{ GeV}$ over-estimation is 150%. Whereas there is an under-estimation of the photon flux when the effect of cavitation is not included in the high p_T regime. E.g., for the following p_T values 1.5, 2.0 and 3.0 (in GeV) under-estimations are around 50%, 65% and 30% respectively.

In Fig.[12] we plot photon production rates for various cavitation times obtained by varying ΔT (with $a = 0.901$ is fixed). Here the enhancement in the photon production when ΔT is reduced to half of its base value is about 75% at $p_T = 0.5 \text{ GeV}$ and about 55% at $p_T = 1 \text{ GeV}$. A further reduction of the parameter value to $\Delta T/4$ is enhancing the photon production by about 120% at $p_T = 0.5 \text{ GeV}$ and about 85% at $p_T = 1 \text{ GeV}$. The reason is a reduction in ΔT amounts to increase in the cavitation time (see e.g., Fig.[6]), which in turn increases the time inter-

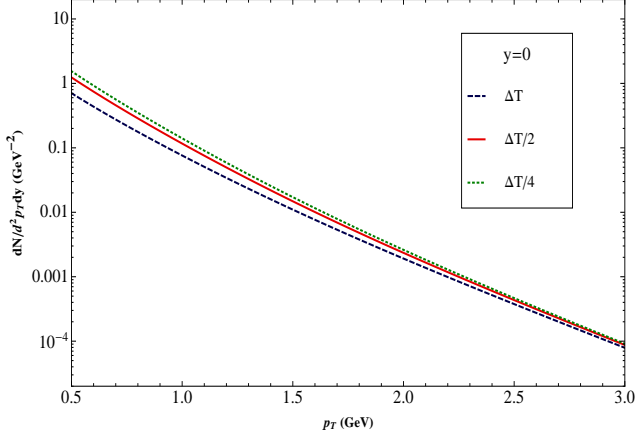


FIG. 12. Photon production rates showing the effect of different cavitation time. Viscous corrections to the distribution functions has been included.

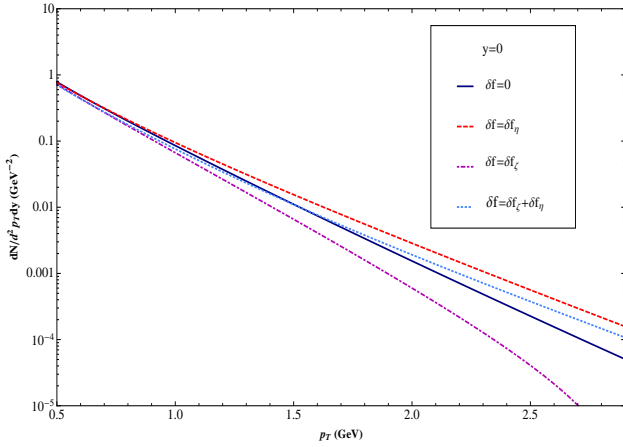


FIG. 13. Viscous corrections to the distribution function and photon production rate. The solid line shows the photon production rate without the viscous corrections to the distribution function and the other lines shows the cases with addition of viscous corrections due to shear and bulk viscosities.

val over which photon production is calculated. Therefore this increases the photon flux.

In Fig.[13] we show the effect of viscous corrections to the distribution function on photon production. Here we consider the cavitation scenario with ΔT ($= T_c/14.5$)

and a ($=0.901$). The solid curve shows the case $\delta f = 0$. We can see from the figure that when we include only the shear viscosity correction ($\delta f = \delta f_\eta$), it enhances the photon production particularly in high p_T regime[18]. Next we consider the corrections arising due to bulk viscosity $\delta f = \delta f_\zeta$ only. The effective pressure due to Π is negative and we have seen that it is crucial for the cavitation to occur (See Eq.[7]). As a result number of particle with higher momenta are decreasing and therefore there is a reduction in photon rate as compared to the case without the viscous correction[62]. As it is clear from the figure, the effect of bulk viscosity is to oppose the contribution from the shear viscosity. The combined effect of both shear and bulk viscosity corrections ($\delta f = \delta f_\eta + \delta f_\zeta$) can be seen in the graph just below the top-most curve. It is clear from the graph that effect of viscous corrections to the distribution functions increases in the high p_T regime.

IV. SUMMARY AND CONCLUSIONS

Using the second order relativistic hydrodynamics we have analyzed the role of non-ideal effects near T_c arising due to the equation of state, bulk-viscosity and cavitation on the thermal photon production from QGP. Since the experiments at RHIC imply extremely small values for η/s , we take the value $1/4\pi$ for shear viscosity. We have shown using non-ideal EoS from the recent lattice results that the hydrodynamical expansion gets significantly slow down as compared to the case with the massless EoS. This, in turn, enhances the flux of hard thermal photons.

Bulk viscosity plays a dual role in heavy-ion collisions: On one hand it enhances the time by which the system attains the critical temperature, while on the other hand it can make the hydrodynamical treatment invalid much before it reaches T_c . Another result we would like to emphasize is that if the viscous correction δf to the distribution function is not included, then ignoring cavitation can lead to a significant over-estimation of the photon production rate. But when the viscous corrections are included the situation can become more complex. In the low p_T regime (<1.1 GeV) there is a significant over-estimation in the photon flux if cavitation is ignored. On the other hand, in the high p_T regime (>1.1 GeV) the photon flux is under-estimated when the cavitation is ignored!

-
- [1] J. Kapusta, P. Lichard and D. Seibert, Phys. Rev. **D 44**, 2774 (1991).
 - [2] R. Baier, H. Nakkagawa, and K. Redlich, Z. Phys. **C 53**, 433 (1992).

- [3] P. V. Ruuskanen, Nucl. Phys. **A 544**, 169c, (1992).
- [4] M. H. Thoma, Phys. Rev. **D 51**, 862, (1995).
- [5] C. T. Traxler, H. Vija, and M. H. Thoma, Phys. Lett. **B 346**, 329 (1995)

- [6] P. Arnold, G. D. Moore and L. G. Yaffe, JHEP **057**, 011 (2001); P. Arnold, G. D. Moore and L. G. Yaffe, JHEP **09**, 012 (2001).
- [7] J. Alam, S. Sarkar, P. Roy, T. Hatsuda and B. Sinha, Ann. Phys. (NY) **286**, 159 (2001).
- [8] T. Peitzmann and M. H. Thoma, Phys. Rept. **364**, 175-246 (2002), arXiv: hep-ph/0111114.
- [9] C. Gale and K. L. Haglin, arXiv: hep-ph/0306098v3.
- [10] J. Kapusta and C. Gale, *Finite Temperature Field Theory*, Cambridge University Press, (2006).
- [11] E. L. Fienberg, Nuovo Cim. **A 34**, 391 (1976)
- [12] E. V. Shuryak, Phys. Lett. **78**, 150 (1978)
- [13] D. K. Srivastava, Eur. Phys. J. **C 10**, 487-490 (1999)
- [14] F. D. Steffen, and M. H. Thoma, Phys. Lett. **B 510**, 98-106 (2001)
- [15] D. K. Srivastava, J. Phys. G: Nucl. Part. Phys. **35**, 104026, (2008).
- [16] F. M. Liu and K. Werner, J. Phys. G: Nucl. Part. Phys. **36**, 035101, (2009).
- [17] J. R. Bhatt and V. Sreekanth, Int. J. Mod. Phys. **E 19**, 299-306, (2010)
- [18] K. Dusling, arXiv:0903.1764 [hep-th]
- [19] T. Schaefer and D. Teaney, Rept. Prog. Phys. **72**, 126001, (2009).
- [20] P. K. Kovtun, D. T. Son and A. O. Starinets, Phys. Rev. Lett. **94**, 111601 (2005)
- [21] T. Hirano and M. Gyulassy, Nucl. Phys. **A769**, 71 (2006).
- [22] K. Adcox *et al.* [PHENIX Collaboration]; Nucl. Phys. **A757**, 184 (2005); B. B. Back *et al.* [PHOBOS Collaboration]; Nucl. Phys. **A757**, 28 (2005); J. Adams *et al.* [STAR Collaboration]; Nucl. Phys. **A757**, 102 (2005); B. Alver *et al.* [PHOBOS Collaboration], Phys. Rev. Lett. **98**, 242302 (2007); B. I. Abelev *et al.* [STAR Collaboration], Phys. Rev. **C 77**, 054901 (2008)
- [23] R. Baier and P. Romatschke, Eur. Phys. J. **C 51**, 677 (2007).
- [24] P. Romatschke and U. Romatschke, Phys. Rev. Lett. **99**, 172301 (2007).
- [25] K. Dusling and D. Teaney, Phys. Rev. **C 77**, 034905 (2008).
- [26] H. Song and U.W. Heinz, Phys. Rev. **C 77**, 064901 (2008).
- [27] M. Luzum and P. Romatschke, Phys. Rev. **C 78**, 034915 (2008) [Erratum-ibid. **C 79**, 039903 (2009)]
- [28] D. Molnar and P. Huovinen, J. Phys. G **35**, 104125 (2008)
- [29] H. Song and U. W. Heinz, arXiv:0812.4274 [nucl-th].
- [30] M. Luzum and P. Romatschke, arXiv:0901.4588 [nucl-th].
- [31] S. Weinberg, *Gravitation and Cosmology*, John Wiley & Sons, (1972).
- [32] A. Bazavov *et al.*, Phys. Rev. **D 80**, 014504 (2009)
- [33] H. B. Meyer, Phys. Rev. Lett. **100**, 162001 (2008)
- [34] R. J. Fries, B. Müller, and A. Schäfer, Phys. Rev. **C 78**, 034913 (2008)
- [35] K. Rajagopal, and N. Tripuraneni, JHEP **1003**, 018 (2010)
- [36] S. de Groot, W. van Leeuwen, and Ch. van Veert, *Relativistic Kinetic Theory*, North-Holland, (1980).
- [37] J. D. Bjorken, Phys. Rev. **D 27**, 140 (1983).
- [38] D. Teaney, Phys. Rev. **C 68**, 034913 (2003).
- [39] U. W. Heinz, H. Song, and A. K. Chaudhuri, Phys. Rev. **C 73**, 034904 (2006).
- [40] A. Muronga, Phys. Rev. **C 76**, 014909 (2007).
- [41] A. Muronga, Phys. Rev. Lett. **88**, 062302 (2002), [Erratum-ibid. **89**, 159901 (2002)].
- [42] W. A. Hiscock and L. Lindblom, Phys. Rev. **D 31**, 725 (1985).
- [43] R. Baier, P. Romatschke, and U. A. Wiedemann, Phys. Rev. **C 73**, 064903 (2006).
- [44] W. Israel, Ann. Phys. **100**, 310 (1976); W. Israel and J. M. Stewart, Ann. Phys. **118**, 341 (1979).
- [45] A. Muronga and D. H. Rischke, (2004) arXiv:nucl-th/0407114.
- [46] P. Romatschke, Int. J. Mod. Phys. **E 19**, 1-53, (2010).
- [47] U. Heinz, arXiv:nucl-th/0512049.
- [48] R. Baier, P. Romatschke, D. T. Son, A. O. Starinets and M. A. Stephanov, JHEP **0804**, 100 (2008).
- [49] M. Natsuume and T. Okamura, Phys. Rev. **D 77**, 066014 (2008).
- [50] S. Bhattacharyya, V. E. Hubeny, S. Minwalla and M. Rangamani, JHEP **0802**, 045 (2008)
- [51] F. Karsch, D. Kharzeev, and K. Tuchin, Phys. Lett. **B 663**, 217 (2008)
- [52] D. Kharzeev and K. Tuchin, JHEP **0809**, 093 (2008)
- [53] G. D. Moore and O. Saremi, JHEP **0809**, 015 (2008) [arXiv:0805.4201[hep-ph]].
- [54] P. Romatschke and D. T. Son, Phys. Rev. **D 80**, 065021 (2009).
- [55] S. Caron-Huot, Phys. Rev. **D 79**, 125009 (2009)
- [56] P. Aurenche, F. Gelis, H. Zaraket, and R. Kobes, Phys. Rev. **D 58**, 085003 (1998)
- [57] F. Karsch, Z. Phys. **C 38**, 147 (1988)
- [58] C. T. Traxler and M. H. Thoma, Phys. Rev. **C 53**, 1348 (1996)
- [59] C. Sasaki and K. Redlich, Phys. Rev. **C 79**, 055207 (2009)
- [60] G. S. Denicol, T. Kodama, T. Koide, and Ph. Mota, Phys. Rev. **C 80**, 064901 (2009)
- [61] P. Bozek, Phys. Rev. **C 81**, 034909 (2010)
- [62] A. Monnai, and T. Hirano, Phys. Rev. **C 80**, 054906 (2009)